Ecological Indicators 131 (2021) 108238

Contents lists available at ScienceDirect

Ecological Indicators

journal homepage: www.elsevier.com/locate/ecolind

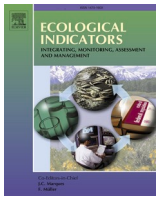

Unlocking Kautsky's dark box: Development of an optical toxicity classification tool (OPTOX index) with marine diatoms exposed to emerging contaminants

Bernardo Duarte [a,b,*], Eduardo Feijão [a], Ricardo Cruz de Carvalho [a,b,c], Marco Franzitta [a], João Carlos Marques [d], Isabel Caçador [a,b], Maria Teresa Cabrita [e], Vanessa F. Fonseca [a,f]

[a] MARE – Marine and Environmental Sciences Centre, Faculty of Sciences of the University of Lisbon, Campo Grande 1749-016 Lisbon, Portugal
[b] Departamento de Biologia Vegetal, Faculdade de Ciências da Universidade de Lisboa, Campo Grande 1749-016, Lisboa, Portugal
[c] Centre for Ecology, Evolution and Environmental Changes (cE3c), Faculdade de Ciências, Universidade de Lisboa, Lisboa 1749-016, Portugal
[d] MARE – Marine and Environmental Sciences Centre, c/o Department of Zoology, Faculty of Sciences and Technology, University of Coimbra, 3000 Coimbra, Portugal
[e] Centro de Estudos Geográficos (CEG), Instituto de Geografia e Ordenamento do Território (IGOT), University of Lisbon, Rua Branca Edmée Marques, 1600-276 Lisbon, Portugal
[f] Departamento de Biologia Animal, Faculdade de Ciências da Universidade de Lisboa, Campo Grande, 1749-016 Lisboa, Portugal

ARTICLE INFO

Keywords:
Chlorophyll *a* induction curves
Marine diatoms
Ecotoxicology
Bio-optical index

ABSTRACT

Chlorophyll *a* induction curves, or Kautsky curves, have been extensively used to study physiological stress conditions in phototrophic organisms, with the analysis of several derived parameters. Nevertheless, these variables use only about 10 % of the information comprised in the complete Kautsky curve dataset, leaving 90 % of the photochemical data within an underutilized dark box, that is not translated into photochemically relevant variables. By observing the variable fluorescence profiles from marine diatoms exposed to a myriad of emerging and classical contaminants, several fluorescence profile alterations were detected, with significant deviations from the control conditions concomitant with the degree of growth inhibition imposed by the chemical stressor. The Linear Discriminant Analysis (LDA) analysis based on the normalized variable chlorophyll *a* fluorescence profiles revealed a high discriminatory efficiency of the type of contaminant to which the cultures were exposed, indicating that the exposure to different chemical stressors (contaminants) results in specific fluorescence profiles that can be used as descriptors of these exposure conditions. Analysing the individual contaminant LDA analysis, a very low overlap between samples exposed to different concentrations was observed, indicating a high discriminatory power of the variable fluorescence profiles. When evaluating the blind-test classification efficiencies, provided by this contaminant-specific LDA approach, it was possible to observe a high degree of efficiency in almost all contaminants tested, and for most of the concentrations applied. With this in mind, the produced linear discriminants and proportion of traces was used to compute an optical toxicity classification tool - the OPTOX index. The index revealed a high degree of correlation with the growth inhibition observed and/or with the exogenous dose of contaminant applied. The developed OPTOX index, a unifying tool enclosing all the fluorescence data provided by the chlorophyll *a* induction curve, proved to be an efficient tool to apply in ecotoxicological assays using marine model diatoms with a high degree of reliability for classifying the exposure of the cells to emerging contaminants. Additionally, the data analysis pipeline, as well as the index development methodology here proposed, can be easily transposed to other autotrophic organisms subjected to different ecotoxicological test conditions calibrated and validated against known biochemical or morphological descriptors of stress, integrating this way a large amount of data that was until know completely overlooked and left within an underutilized and undervalued dark box.

* Corresponding author.
E-mail address: baduarte@fc.ul.pt (B. Duarte).

https://doi.org/10.1016/j.ecolind.2021.108238
Received 15 August 2021; Received in revised form 24 September 2021; Accepted 25 September 2021
Available online 28 September 2021

1. Introduction

Since the industrial revolution, trace elements have been dumped into coastal areas as a result of increased anthropogenic activity, becoming a legacy for estuarine and coastal environments (Duarte et al., 2013). Despite the industrial activity with lower environmental impact in the last decades, there is an evident increase in the development of uncontrolled human activities (Gavrilescu et al., 2015), and the relationship between human population density and environmental changes in coastal regions is well known. The EU's Task Group for the Marine Strategy Framework Directive implementation recommended that monitoring programs covering the concentration of chemical contaminants should also integrate biological measurements of their effects on marine organisms (Law et al., 2010). The combination of conventional and newer effect-based methodologies, with the assessment of environmental contaminant concentrations, provides a powerful and comprehensive approach (Law et al., 2010). It is also striking that the pace of chemical discovery is growing rapidly, with the Chemicals Abstracts Service reporting in May 2011 the registration of the 60th million chemical substance, while the 50th million substance was registered in 2009, highlighting the continued acceleration of synthetic chemical innovation (CAS, 2011). Allied to this rapid development in the discovery and production of new chemical compounds comes an emerging cost. A burst of organic chemical contaminants is now of major concern, not due to their high environmental concentrations but to their striking impact, even at low concentrations. Their rise is so evident, that these contaminants are now ubiquitous in marine waters, from large urbanized estuaries (Reis-Santos et al., 2018) to remote oceanic locations, tens of thousands of km away from the nearest settled population (Duarte et al., 2021b). For example, pesticides continue to be detected in surface and ground waters (Duarte et al., 2021b), and pharmaceuticals, concentrated in wastewaters, are permanently discharged from medical facilities and households, ending up in coastal areas (Fonseca et al., 2020; Reis-Santos et al., 2018), while personal care products with widespread use have been detected in phytoplankton cells in Antarctica (Duarte et al., 2021b). Moreover, these compounds are often designed to be resistant to biological degradation and to target specific biological or cellular agents, and thus not only do they persist in the environment roving through the system (Fonseca et al., 2020), but also have severe target effects in living organisms (Cruz de Carvalho et al., 2020b; Duarte et al., 2020; Feijão et al., 2020). Among the multitude of emerging contaminants, several have raised concerns due to their ecotoxicological effects and how to assess them efficiently. Acumen dictates a multidisciplinary approach, but often a truly comprehensive framework, from xenobiotic internalization, mode-of-action, triggered molecular pathways, physiological responses, to the exploration of big data and intertwined responses, is hard to grasp, but excitingly within reach. In this context, it is paramount that we develop new integrated ecotoxicological methodologies for the evaluation of the impacts of new emerging contaminants in marine organisms.

Phototrophs are at the basis of all marine ecosystems, cycling solar energy and soaking carbon, fuelling the trophic web. Any disruption at this level has expected impacts on the whole marine ecosystem. Contaminants toxicity are known to have negative and specific impacts on these organisms, especially at their photochemical apparatus level (Duarte et al., 2021c, 2021a; Feijão et al., 2020; Franzitta, 2020). With both biochemical and biophysical components, these organisms allow for the photosynthetic mechanisms to be addressed remotely (Anjum et al., 2016). Bio-optical techniques such as Pulse Amplitude Modulated (PAM) fluorometry emerge as potential non-invasive high-throughput screening (HTS) tools (Duarte et al., 2021c, 2021a). These tools use optical signatures as a proxy of the phototroph physiology, allowing for the detection of any disturbances at the primary productivity level (Cabrita et al., 2018), which have proved to efficiently evaluate contaminants' effects with a dose-related response (Santos et al., 2014) and be included in numerical indexes, easily conveyed to stakeholders (Cruz de Carvalho et al., 2020a; Duarte et al., 2021a). The integrated repeated measures over time without organism scarification is another key benefit of this approach. This is the cornerstone of the pioneering research field of toxicophenomics, merging plant phenomics, that aims to measure traits such as growth and performance of plants using non-invasive technologies, with ecotoxicology, shifting the use of these phenotyping tools to address contaminant induced stress in autotrophs. The application of optical techniques to disclose different groups of samples exposed to different degrees of contamination has already been applied in marine phototrophs with a high degree of efficiency, in ecotoxicological trials and under field conditions (Cruz de Carvalho et al., 2020a; Duarte et al., 2021a), and using mixed organisms samples in opposition to single species, with also a high degree of efficiency in detecting responses to contaminants (Duarte et al., 2018). The application of these bio-optical technologies produces large datasets with physiological interest, depicting the effects of a given compound on an autotrophic organism, which can also be explored by multivariate statistical approaches and machine learning techniques aiming to produce classifiers of the degree of toxicity to which organisms are exposed (Rodrigues et al., 2021).

The so-called JIP test, resultant from the chlorophyll *a* fluorescence induction curves, produces a large amount of fluorescence data (more than 400 fluorescence data points) and depicting the Kautsky effects and reflecting the whole photochemical process from the moment a photon hits the Photosystem II (PSII) antennae to its conversion into electron potential, transport through the electron transport chain (ETC) until it reaches the Photosystem I (PSI) (Stirbet et al., 2018; Stirbet and Govindjee, 2011). Nevertheless, from these large datasets normally only a very low amount of fluorescence data points is used for calculating physiological relevant variables that reflect specific photochemical processes (Stirbet and Govindjee, 2011; Strasser et al., 2004, 2000), leaving out a high amount of data points, with potential as classifiers of the stress imposed, in a neglected dark box. In previous works, we have demonstrated that the application of the whole chlorophyll *a* fluorescence induction curves can generate canonical groupings of samples under different types of stresses including contaminants (Cruz de Carvalho et al., 2020b; B. Duarte et al., 2020a; Duarte et al., 2021c, 2021a; Feijão et al., 2020; Silva et al., 2020). Although this provided a clear way to separate samples exposed to different doses, this canonical technique did not provide any means to integrate the whole fluorescence dataset into a single integrative value to classify the samples for ecotoxicological porpoises.

Therefore, the present work aims to disclose the potential of this fluorescence dark box, by applying the whole chlorophyll *a* fluorescence induction curves dataset into a classifying tool (Optical Toxicity Classification Index, OPTOX-index), applicable to ecotoxicological assessment using model marine diatoms (*Phaeodactylum tricornutum*) exposed to relevant emerging contaminants of concern.

2. Material and methods

2.1. Ecotoxicological trials

Phaeodactylum tricornutum cells, obtained from axenic cultures, were grown in f/2 medium (Guillard and Ryther, 1962) under asexual reproduction at temperature-controlled conditions (18 ± 1 °C), constant aeration, and under a 14-h light/10-h dark cycle provided by a LED light source (FytoScope Chamber FS 130 (Photon Systems Instruments, Czech Republic), 80 μmol photons m^{-2} s^{-1}). Light intensity was measured using the photosynthetic active radiation (PAR) sensor available in FluorPen FP100 (Photon System Instruments, Czech Republic). For contaminant exposure, the guidelines from the Organization for Economic Cooperation and Development (OECD) for algae bioassays were used (OECD, 2011). Relatively low initial cell density (4×10^{-5} cell mL^{-1}) was used in these experiments, following the previously mentioned OECD guidelines (OECD, 2011), for microalgae cells with

similar size to *P. tricornutum*, and also to better reflect cell concentrations found in marine coastal areas. All exposure experiments were carried out in 500 mL Schott washing flasks under the abovementioned abiotic conditions in phytoclimatic chambers. Following inoculation, cells were left to grow for 48 h before being exposed to the contaminant for an additional 48 h period, allowing this way an exposure only during the exponential phase of cell growth. This methodology was previously employed proving effective to avoid possible artefacts due to culture ageing (Cruz de Carvalho et al., 2020b; Duarte et al., 2020a; Feijão et al., 2020; Franzitta, 2020; Silva et al., 2020). Exposure compounds and doses (Table 1) used were chosen according to their environmental relevance and available literature regarding potential toxic effects in this or other related species (Cruz de Carvalho et al., 2020b; Duarte et al., 2020a; Fabbri and Franzellitti, 2016; Feijão et al., 2020; Franzitta, 2020; Reis-Santos et al., 2018; Silva et al., 2020). Exposure was performed by diluting a suitable volume of the contaminant stock solution into the growth medium. Culture growth was monitored using PAM fluorometry and calibrated growth curves for this particular species (Feijão et al., 2018). Growth inhibition was used as a toxicity proxy and was calculated according to Eqs. (1) and (2) following the OECD guidelines (OECD, 2011):

$$\mu_{i-j} = \frac{\ln B_j - \ln B_i}{t_j - t_i} \quad (1)$$

where $\mu_{i\text{-}j}$ is the average specific growth rate from moment time i to j; t_i is the moment time for the start of the period; t_j is the moment time for end of the period; Bj and Bi is the cell density at time j and I respectively.

$$Growth\ Inhibition(\%) = \frac{\mu_C - \mu_T}{\mu_C} \quad (2)$$

where μ_C is the average specific growth rate of the control and μ_T is the average specific growth rate of the treatment condition.

Table 1
Tested contaminants and respective concentrations used in the *Phaeodactylum tricornutum* ecotoxicological trials.

Contaminant	Treatment	Concentration
A. Diclofenac	C1	0.8 μg L^{-1}
	C2	3 μg L^{-1}
	C3	40 μg L^{-1}
	C4	100 μg L^{-1}
	C5	300 μg L^{-1}
B. Ibuprofen	C1	0.8 μg L^{-1}
	C2	3 μg L^{-1}
	C3	40 μg L^{-1}
	C4	100 μg L^{-1}
	C5	300 μg L^{-1}
C. Propranolol	C1	0.3 μg L^{-1}
	C2	8 μg L^{-1}
	C3	80 μg L^{-1}
	C4	150 μg L^{-1}
	C5	300 μg L^{-1}
D. Fluoxetine	C1	0.3 μg L^{-1}
	C2	0.6 μg L^{-1}
	C3	20 μg L^{-1}
	C4	40 μg L^{-1}
	C5	80 μg L^{-1}
E. Glyphosate	C1	10 μg L^{-1}
	C2	50 μg L^{-1}
	C3	100 μg L^{-1}
	C4	250 μg L^{-1}
	C5	500 μg L^{-1}
F. Sodium dodecyl sulphate (SDS)	C1	0.1 mg L^{-1}
	C2	1 mg L^{-1}
	C3	3 mg L^{-1}
	C4	10 mg L^{-1}
G. Triclosan	C1	0.1 μg L^{-1}
	C2	1 μg L^{-1}
	C3	10 μg L^{-1}
	C4	50 μg L^{-1}
	C5	100 μg L^{-1}
H. Dissolved Cu	C1	1 μg L^{-1}
	C2	5 μg L^{-1}
	C3	10 μg L^{-1}
I. Cu nanoparticle (NP)	C1	1 μg L^{-1}
	C2	5 μg L^{-1}
	C3	10 μg L^{-1}

2.2. Chlorophyll *a* fluorescence induction curves

At the end of the 48-h exposure period, liquid samples were harvested and transferred to 3 mL cuvettes (N = 30) and dark-adapted for 15 min before PAM fluorometry measurements. Chlorophyll *a* fluorescence induction curves or Kautsky effect were measured according to the pre-programmed FluorPen FP100 (Photon System Instruments, Czech Republic) OJIP protocol. Briefly, a dark-adapted sample is exposed to a modulated saturating light intensity of 3500 μmol photons m^{-2} s^{-1}, generating a polyphasic rise in fluorescence known as Kautsky Effect or curve. The chlorophyll fast induction kinetics or Kautsky curve depicts the rate of reduction kinetics of various components of PS II. The resultant fluorometric analysis produces 456 fluorescence data points per fluorometric measurement.

2.3. Data analysis

To avoid potential artefacts from the impossibility of performing such a large number of incubations in a contemporaneous form, the fluorescence data of each incubation set was normalized by calculating the difference in relative variable fluorescence towards the respective and contemporaneous control fluorescence values, allowing for variation towards the control to be represented as ΔV curves, using a previously successfully employed normalization procedure (Eq. (3)):

$$V_t = \frac{F_t - F_o}{F_M - F_t} \quad (3)$$

where, V_t is the variable fluorescence measured in a sample replicate at the time t of the Kautsky curve, F_t is the fluorescence measured at the time t of the Kautsky curve, F_o and $F_M$are respectively the basal (fluorescence at time 0) and maximum fluorescence (maximum attained fluorescence during the induction curve) of the same sample replicate. Subsequentially, the following Eq. (4) was used:

$$\Delta V_t = V_t(treatment) - \overline{V_t(control)} \quad (4)$$

where ΔV_t is the normalized variable fluorescence at time referent to the values determined as above, for a specific time t of the Kautsky curve, $V_t(treatment)$ is the variable fluorescence at the time t of the Kautsky curve calculated for a certain sample replicate exposed at a certain contaminant at a specific dose, and $\overline{V_t(control)}$ is the average variable fluorescence calculated for a time t of the Kautsky curve in the contemporaneous control samples.

Linear discriminant analysis (LDA) was performed in R-Studio using the *mass* and *caret* packages for machine learning workflow. Linear discriminant analysis bidimensional plots were constructed using the *tidyverse* package for data manipulation and visualization. Normalized variable fluorescence variation (ΔV_t) data was used for all LDA analyses. To setup, the training and test datasets for all discriminant analysis, the sample sets were divided into 40% of the samples data used for model training, and the remaining 60% of the samples data was used for the model test. The application of training and blind test phases allows for the calculation of the efficiency of the models in both LDA phases, by evaluating the number of samples classified in the correct group (contaminant treatment). The LDA model uses the training dataset to model a linear combination of features that characterizes or separates two or more classes of objects or events, while testing their correct attribution to the treatment groups defined. The test set is used to

perform a blind classification of the samples using the model produced in the training session, to evaluate the model efficiency in classifying blindly a totally independent dataset into the correct treatment categories.

The Optical Toxicity classification index (OPTOX-Index, Eq. (3)) was built using the normalized variable fluorescence data and the attained linear discriminants (LD_n) produced in the LDA analysis for each contaminant, weighted by the proportion of trace (percentage separation achieved by each discriminant function, PT_{LD_n}):

$$OPTOX - Index = \sum \Delta V_t \times LD_1(t) \times PT_{LD_1} + \cdots + \Delta V_t \times LD_n(t) \times PT_{LD_n} \quad (5)$$

where $LD_n(t)$ is the linear discriminant n relative to the normalized variable fluorescence (ΔV_t), measured at time t. The OPTOX-Index of certain sample results from the sum of the abovementioned formula results for all the fluorescence timesteps (variables, from t = 0 to t = 1991621 μs) of the analysed sample.

Spearman correlation coefficients and statistical significance between the index, exogenous concentration and growth inhibition values were computed using the *corrplot* package in R-Studio Version 1.4.1717. Violin plots Non-parametric Kruskal-Wallis with Bonferroni *post-hoc* were performed using the *agricolae* package in R-Studio Version 1.4.1717. Violin plots with probability density of the data at different values smoothed by a kernel density estimator were computed and plotted using *ggplot2* along with the classical boxplot package in R-Studio Version 1.4.1717.

3. Results

3.1. Growth inhibition

The growth inhibition of the test cultures towards their respective control conditions (Fig. 1), shows that the application of the test substances leads to substantial decreases in cell density at the highest concentrations applied. This was more evident in the cultures exposed to ibuprofen (Fig. 1B), propranolol (Fig. 1C), fluoxetine (Fig. 1D), glyphosate (Fig. 1E) and SDS (Fig. 1F). In the cultures exposed to diclofenac, a biphasic response was detected, with intermediate concentrations of this pharmaceutical compound leading to more pronounced growth inhibition than in the cells exposed to higher concentrations. Regarding the cultures exposed to triclosan and Cu (Fig. 1G, H and I) an increasing trend was observed, with the increasing number of measurements resulting in higher growth inhibitions with increasing concentrations.

3.2. Normalized Kautsky plots (ΔVt)

The normalized Kautsky plots (Fig. 1) revealed changes in the overall fluorescence profile with exposure to various contaminants. This was more pronounced in the initial to the middle phases of the fluorescence profiles (around 10^3 ms) and again in the final fluorescence phase (between 10^5 and 10^6 ms). Moreover, changes were more evident in the curves corresponding to the highest tested concentrations, and specifically in the cultures exposed to ibuprofen (Fig. 2B), propranolol (Fig. 2C), fluoxetine (Fig. 2D), SDS (Fig. 2F) and both Cu forms (Fig. 2H and 2I). This normalization towards the control allows for the elimination of experimental artefacts linked to the non-contemporary experimental setups. By normalizing each test setup towards its contemporary control condition, it reflects and eliminates environmental differences in the test environment among treatments, allowing for direct comparisons. These differential normalized fluorescence profiles, with very different inflexion points at different points of the Vt curves, already point out significant differences between the photochemical echoes attained from the marine diatoms exposed to different emerging contaminants and at different exogenous concentrations.

3.3. Xenobiotic classification

As a first approach, the potential of the normalized Vt curves for the separation of different samples exposed to different emerging

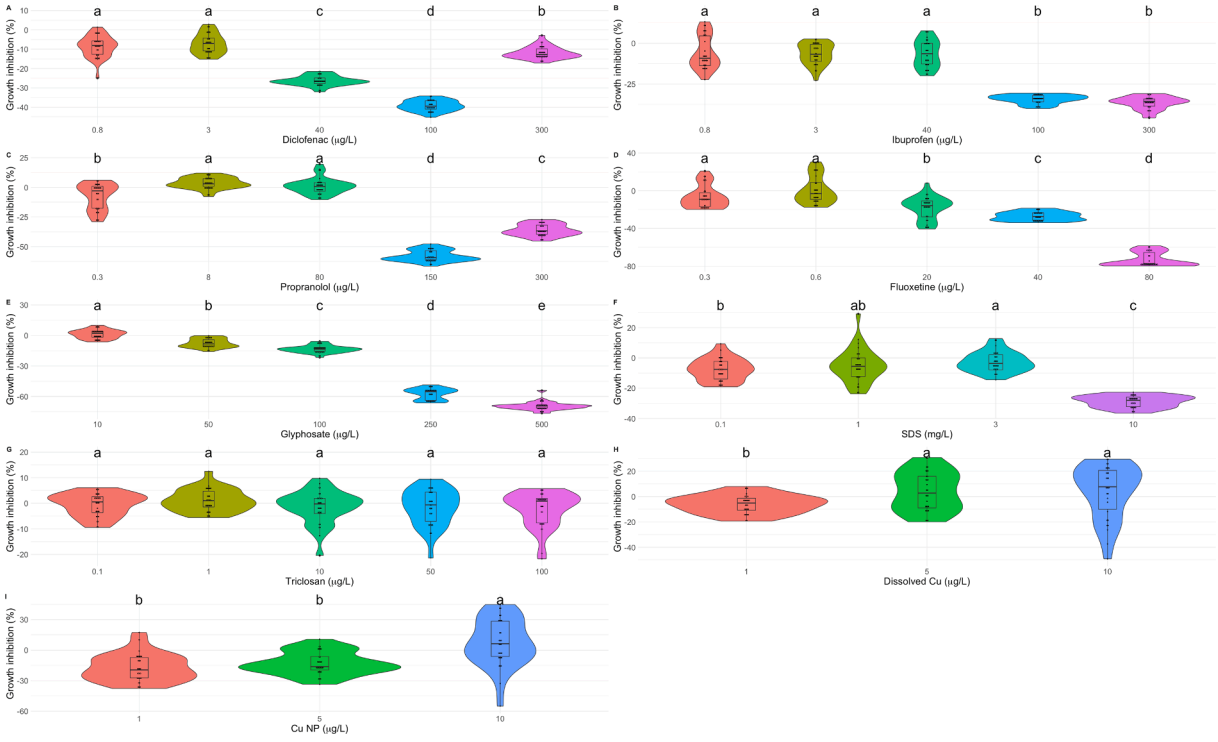

Fig. 1. Violin plots of *Phaeodactylum tricornutum* growth inhibition when compared with the respective control condition (absence of xenobiotic) and under exposure to diclofenac (A), ibuprofen (B), propranolol (C), fluoxetine (D), glyphosate (E), SDS (F), triclosan (G), dissolved Cu (H) and Cu nanoparticle (I) (N = 30 per treatment and per exposure concentration, letters denote pairwise significant differences between treatments at $p < 0.05$).

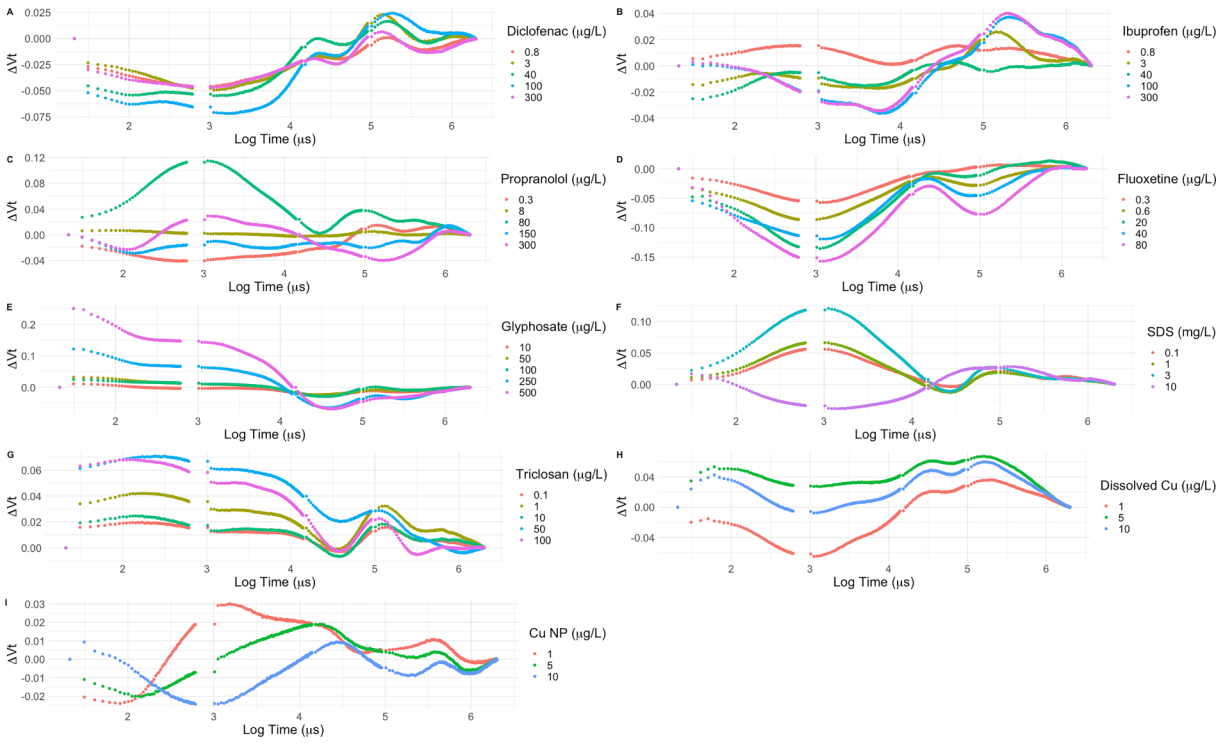

Fig. 2. Normalized variable fluorescence curves (ΔVt), following chlorophyll *a* fluorescence induction curves of *Phaeodactylum tricornutum* cultures under exposure to diclofenac (A), ibuprofen (B), propranolol (C), fluoxetine (D), glyphosate (E), SDS (F), triclosan (G), dissolved Cu (H) and Cu nanoparticle (I) (N = 30 per treatment and per exposure concentration).

contaminants was tested (Fig. 3). Although the apparent overlap in the LDA projection (Fig. 4A), generally high training and test efficiencies could be detected. Regarding the LDA dispersion, the first interesting aspect of notice is the clear separation of the fluorescence data from the samples exposed to dissolved Cu treatments. Also, the samples exposed to diclofenac presented a reduced spatial LDA projection overlap. Albeit the remaining test groups fluorescence data appear to overlap in the LDA plot, this results from a graphical projection artefact, as the classification

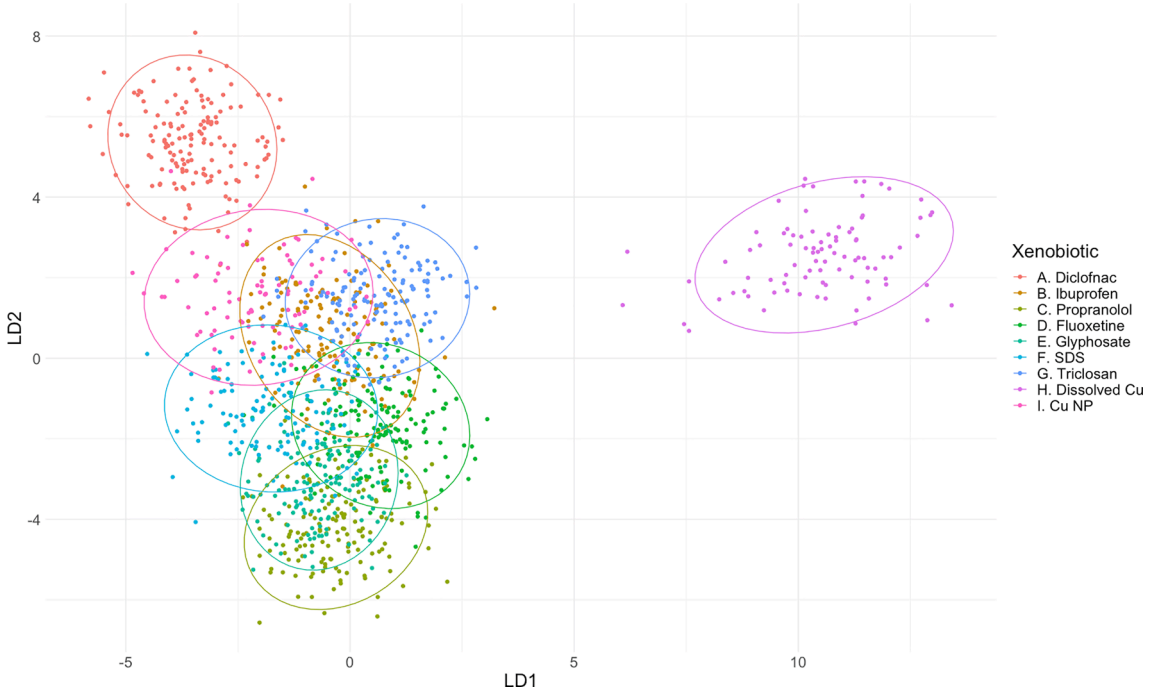

Fig. 3. Linear Discriminant Analysis (LDA) plot based in the chlorophyll *a* fluorescence normalized variable fluorescence curves (ΔVt) datapoints grouped by xenobiotic type, of the *Phaeodactylum tricornutum* cultures exposed to diclofenac (A), ibuprofen (B), propranolol (C), fluoxetine (D), glyphosate (E), SDS (F), triclosan (G), dissolved Cu (H) and Cu nanoparticle (I) (N = 30 per treatment and per exposure concentration; see Table 1 for details). Statistically generated ellipses gather the datapoints within a 95% prediction range.

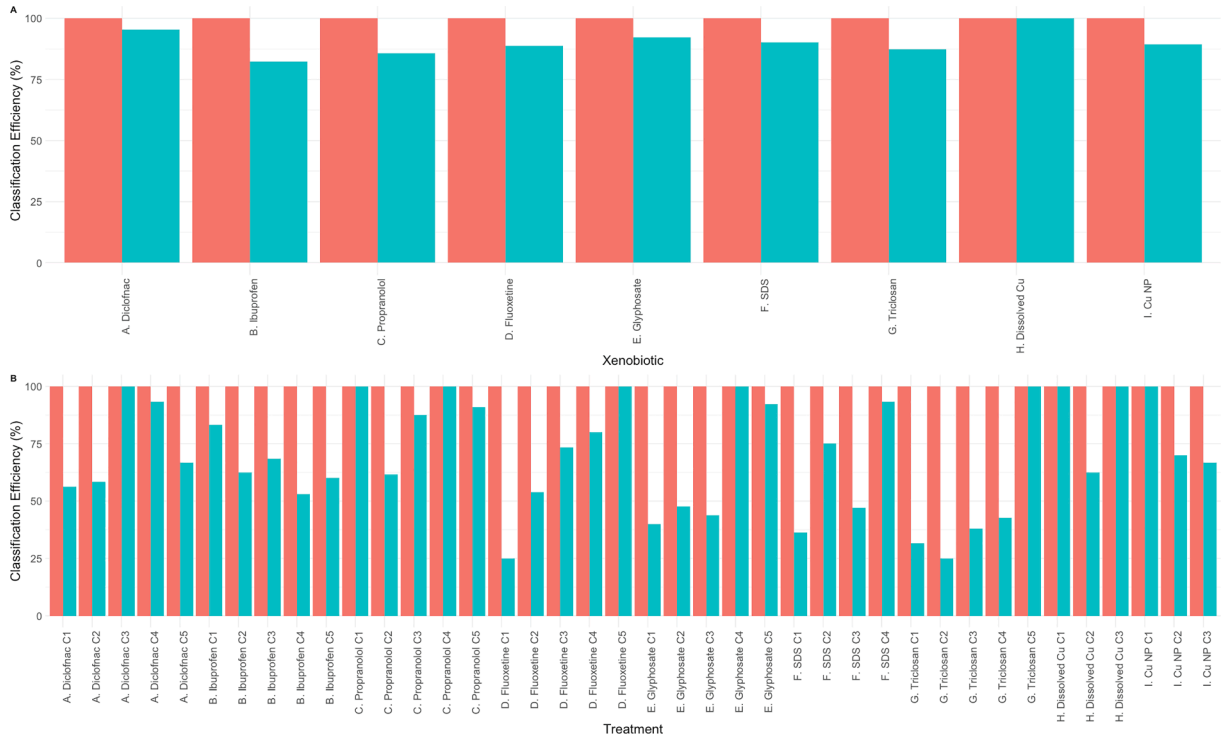

Fig. 4. Linear Discriminant Analysis (LDA) training and test classification efficiency having as input the normalized variable fluorescence curves (ΔVt) chlorophyll *a* fluorescence induction curves of the *Phaeodactylum tricornutum* cultures under the exposure to all xenobiotics with pooled (A) and individual (B) concentrations (N = 30 per treatment and per exposure concentration).

efficiency of the samples regarding the emerging contaminants to which they were subjected always presented values above 75% during LDA test trials indicating a high efficiency of the normalized variable fluorescence curves data as descriptors of the cells physiological state under different exposures (Fig. 4A).

When applying the same LDA approach with the samples grouped by the emerging contaminant and their respective concentration treatment (Fig. 5), higher discrimination of the sample groups was achieved. Once

Fig. 5. Linear Discriminant Analysis (LDA) plot based in the chlorophyll *a* fluorescence normalized variable fluorescence curves (ΔVt) datapoints of the *Phaeodactylum tricornutum* cultures exposed to all tested xenobiotics and concentrations tested individually (N = 30 per treatment and per exposure concentration; see table 1 for details). Statistically generated ellipses gather the datapoints within a 95% prediction range.

again, the samples exposed to the highest concentrations of dissolved Cu appear in a distinct and separate group. Using this approach focusing not only on the xenobiotic type but also on the concentration applied some additional treatments also appear as separate groups. This is the case of the samples exposed to the highest glyphosate, fluoxetine, and diclofenac concentrations. Akin to what was observed in the first LDA analysis, where all the samples were pooled according to the contaminant to which they were exposed, there is an apparent overlap of several sample groups, likely resultant from a spatial projection graphical artefact as can be observed by the high classification efficiencies attained (Fig. 4B). In the LDA training session, all sample groups exhibited a high classification efficiency, whilst in the test session, some sample groups exhibited lower classification efficiencies when their normalized fluorescence values were used as inputs. Nevertheless, most of the classification efficiencies in the LDA test sessions were above 50%, with 42% (17 out of 20) of the sample groups presenting test classification efficiencies above 75% (Fig. 4B). Notably, the lower test classification efficiencies were observed in the lowest exposure concentrations.

3.4. Exposure dose classification

The LDA plots produced for each contaminant clearly shows the effect of the individual doses tested (Fig. 6). In most exposure trials, the normalized variable fluorescence curves data results in LDA groups with a low degree of overlap in the LDA plots. Nevertheless, some overlap can be detected between some of the lower concentrations applied in the plots correspondent to the fluorescence data from cultures exposed to propranolol, glyphosate and triclosan (Fig. 6C, E and G), as well as in the cultures exposed to intermediate concentrations of fluoxetine and SDS (Fig. 6D and 6F respectively). Observing the training and test classification efficiencies of the produced LDAs (Fig. 7) it is possible to observe that all training sessions had very high classification efficiencies with 100% classification efficiencies in almost all contaminants and concentrations. Although with lower classification efficiencies, it is also possible to observe that in most of the emerging contaminants the produced LDA models also presented a very high-test classification efficiency, with values in most of the cases above 75% of efficiency. The exceptions were in the groups representing cultures exposed to low doses of triclosan (Fig. 7G), and in the classification of the different doses of dissolved and nanoparticle Cu forms and concentrations (Fig. 7H). This was also detected in the LDAs produced from the normalized variable fluorescence curves data attained from the cultures exposed to intermediate doses of ibuprofen, glyphosate and SDS (Fig. 7B, E and F respectively).

3.5. LDA-based index

Using the linear discriminants produced from each of the LDA plots (Fig. 6), as well as the proportion of traces (the percentage separation achieved by each discriminant function), it was possible to calculate a weighting value for each variable (normalized variable fluorescence at each measurement time step) to be integrated into a unifying classification index value. The violin plots attained for the calculated index values (considering 30 replicates per treatment) show a clear and common increasing tendency of the index value along with the increasing exogenous dose applied of emerging contaminants (Fig. 8). Additionally, it is possible to notice that the overlap between some of the exposure groups in the LDA plots (indicative of similar fluorescence curve traits), is also well patent in the index values, resulting in very similar index values for overlapping groups.

To validate the applicability and efficiency of the proposed index in reflecting the treatment to which the cultures were subjected, the calculated index values were compared with the exogenous dose concentrations and with the verified growth inhibition percentage for each of the tested contaminants and concentrations (Fig. 9). In all cases the index value presented high correlation coefficients with the exogenous dose applied, being this highly significant in the case of the cultures exposed to fluoxetine, glyphosate, SDS and triclosan (Spearman tests).

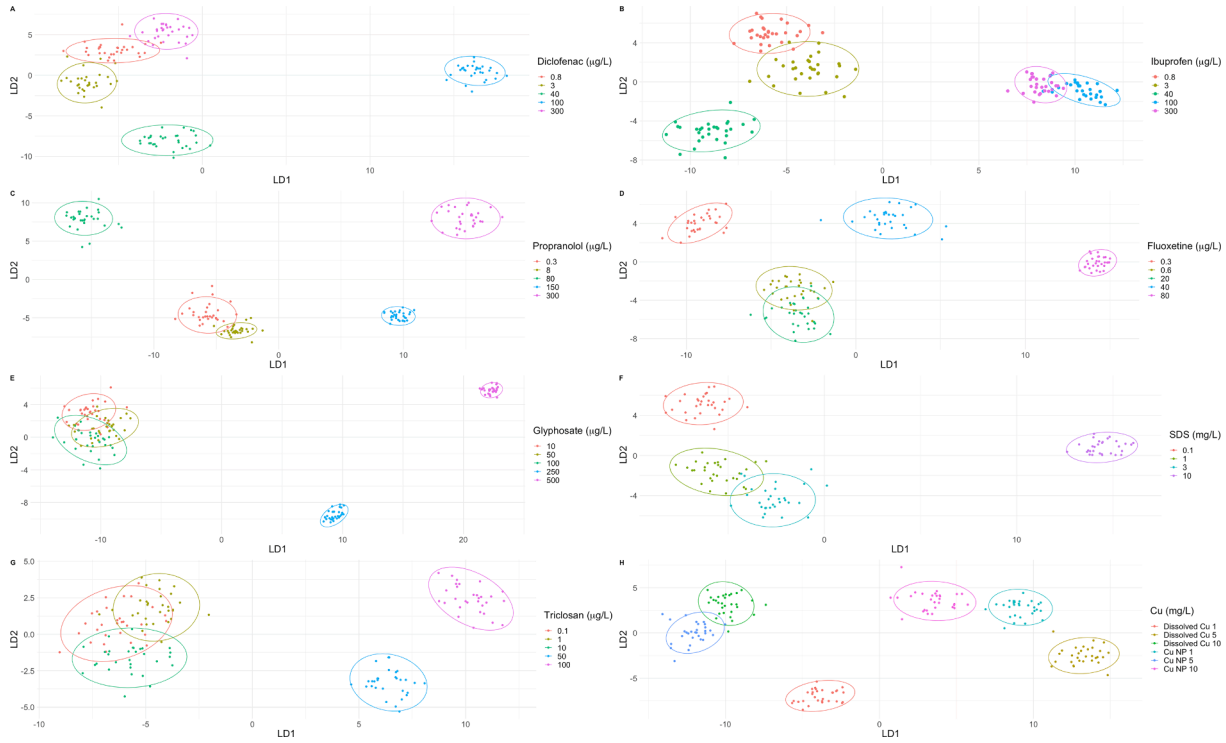

Fig. 6. Individual Linear Discriminant Analysis (LDA) plots based in the chlorophyll *a* fluorescence normalized variable fluorescence curves (ΔVt) datapoints of the *Phaeodactylum tricornutum* cultures exposed to diclofenac (A), ibuprofen (B), propranolol (C), fluoxetine (D), glyphosate (E), SDS (F), triclosan (G), dissolved and nanoparticle Cu (H) and corresponding tested concentrations (N = 30 per treatment and per exposure concentration). Statistically generated ellipses gather the datapoints within a 95% prediction range.

Fig. 7. Linear Discriminant Analysis (LDA) training and test classification efficiency based in the chlorophyll *a* fluorescence normalized variable fluorescence curves (ΔVt) datapoints of the *Phaeodactylum tricornutum* cultures to diclofenac (A), ibuprofen (B), propranolol (C), fluoxetine (D), glyphosate (E), SDS (F), triclosan (G), dissolved Cu (H) and Cu nanoparticle (I) (N = 30 per treatment and per exposure concentration).

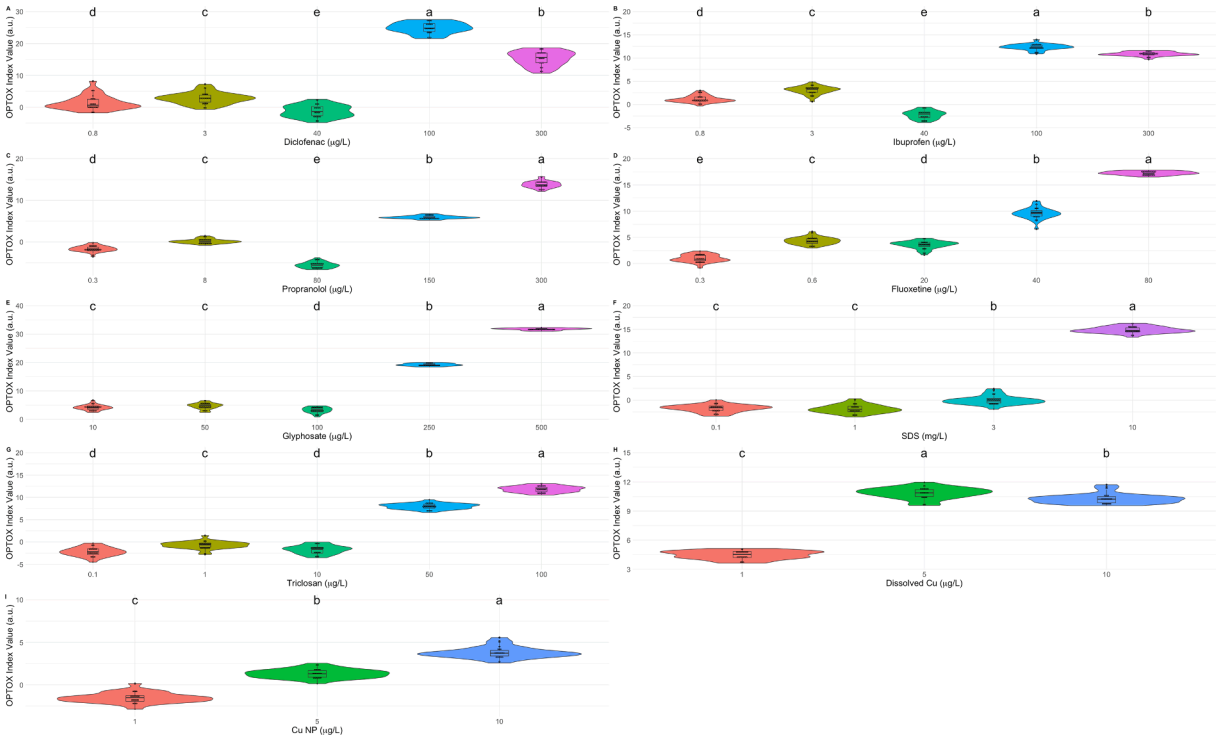

Fig. 8. Linear Discriminant based index (in arbitrary units, a.u.) values violin plots relative to the *Phaeodactylum tricornutum* cultures under the exposure to diclofenac (A), ibuprofen (B), propranolol (C), fluoxetine (D), glyphosate (E), SDS (F), triclosan (G), dissolved Cu (H) and Cu nanoparticle (I) and corresponding tested concentrations (N = 30 per treatment and per exposure concentration, letters denote pairwise significant differences between treatments at $p < 0.05$).

When comparing the index values with the growth inhibition values, it is possible to observe a clear inverse correlation pattern, due to the negative nature of the growth inhibition (highly negative values corresponding to severe growth inhibitions). This was particularly significant in the case of the cultures exposed to fluoxetine, propranolol, glyphosate and SDS.

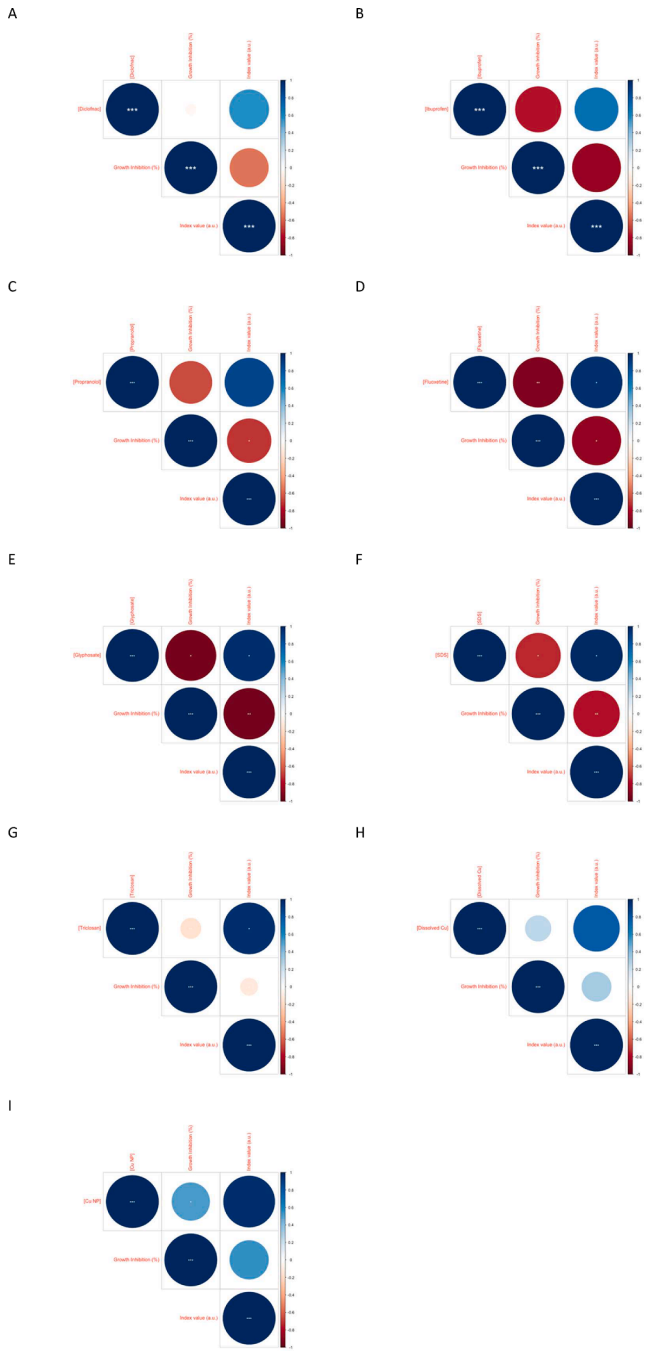

Fig. 9. Spearman correlation coefficients correlograms between the linear discriminant-based index (in arbitrary units, a.u.)and the growth inhibition and exogenous xenobiotic concentration applied of the *Phaeodactylum tricornutum* cultures under the exposure to diclofenac (A), ibuprofen (B), propranolol (C), fluoxetine (D), glyphosate (E), SDS (F), triclosan (G), dissolved Cu (H) and Cu nanoparticle (I) and corresponding tested concentrations (N = 30 per treatment and per exposure concentration, asterisks denote significant correlations at * $p < 0.05$, ** $p < 0.01$, *** $p < 0.001$). Size and colour of the circles are proportional to the Spearman correlation coefficients.

4. Discussion

Chlorophyll *a* induction curves, also commonly known as Kautsky curves, have been widely studied for the assessment of physiological stress in autotrophic organisms, through the use of its derived parameters linked to specific photo-physiological mechanisms and traits (see e.g. Duarte et al., 2020a; Duarte et al., 2015; Kalaji et al., 2011; Tsimilli-Michael et al., 2000; Yan et al., 2012). The application of these Kautsky curves-derived variables for distinguishing among test groups subjected to different stress degrees has been proved in the past, and provided reliable and efficient descriptors and clear statistical separations (Duarte et al., 2021c). These variables present a high physiological value and provide key insights into the mode of action of the applied stress in the test organism. Nevertheless, these variables use only about 10% of the information comprised in the complete Kautsky curve dataset (Strasser et al., 2000). This leaves 90 % of the photochemical data unrealised in a dark box with potentially important information, that is not translated into photochemically relevant variables. Still, in the past, it was also demonstrated that the whole fluorescence profile (comprising the Kautsky curves complete fluorescence dataset) can be included in multivariate statistical approaches, providing very good classification efficiencies with the autotroph groups exposed to different degrees of stress, from either natural (e.g. Duarte et al., 2020b; Duarte et al., 2017; Feijão et al., 2018)) or anthropogenic origin (e.g. Duarte et al., 2020a; Duarte et al., 2021c; Feijão et al., 2020; Franzitta, 2020). Moreover, these datasets have been used in their full extension in artificial intelligence approaches, allowing for the discrimination of sample groups with high accuracy, including the autotroph genotype (Marques da Silva et al., 2020). In a more applied perspective, it is also important that these large photochemical datasets can be translated into unifying values or classification indexes, which can be easily applied, not only by less experienced photophysiologists, but also by other end-users, as diagnostic and monitoring tools. The integration of photochemical variables into unifying indexes has been successfully employed in the recent past, using JIP-derived variables as inputs providing very good classifications of the autotroph stress levels, in both field and experimental conditions (Cruz de Carvalho et al., 2020a; Duarte et al., 2021a, 2017). This approach has been even highlighted by some of the world highly recognized photophysiologists (Stirbet et al., 2018). Nevertheless, and to our knowledge, no index development approach was undertaken until today using the whole Kautsky curve fluorescence dataset.

From an ecotoxicological perspective, the development of such an integrative fluorescence index would be an added value to ecotoxicological tests using autotrophic organisms. By the observation of the variable fluorescence profiles, attained from the marine diatom cultures exposed to a myriad of emerging contaminants, several fluorescence profile alterations were observed in the present study. Moreover, it is possible to observe that this profile deviation towards a control condition is as severe as the growth inhibition observed in the cultures exposed to different contaminants and concentrations. This was expected, as these contaminants are known to induce severe biochemical and photobiological damage in marine diatoms (Cruz de Carvalho et al., 2020b; Duarte et al., 2020a; Duarte et al., 2019; Feijão et al., 2020; Franzitta, 2020; Silva et al., 2020). Beyond the physiological impacts mentioned, studied, and disclosed in the aforementioned references, this tendency opens a new door for the application of fluorescence datasets into a diagnostic/classification ecotoxicological tool. As a first approach, linear discriminant analysis was used to test the power and resolution of this technique for classification of the whole sample dataset regarding the type of exposure to which the diatoms were subjected. The LDA analysis allowed for a blind test classification of the samples in what concerns the contaminant to which samples were exposed, with efficiencies above 75% in all cases. This indicates that the exposure to different chemical stressors (contaminants) results in specific fluorescence profiles that can be used as descriptors of these exposure conditions. This aligns with the different modes of action that these contaminants have in the diatom cells, already described in previous studies (Cruz de Carvalho et al., 2020b; Duarte et al., 2020a; Duarte et al., 2019; Feijão et al., 2020; Franzitta, 2020; Silva et al., 2020). Although with different degrees of inhibition all the tested contaminants resulted in an impairment of specific parts of the photochemical process, being this more evident in the cells exposed to glyphosate and fluoxetine

and with less pronounced effects in the cells exposed to Cu and ibuprofen (Cruz de Carvalho et al., 2020b; Feijão et al., 2020; Franzitta, 2020; Silva et al., 2020). It is also noticed that dissolved Cu exposure leads to a highly differentiated fluorescence profile that is readily highlighted when all contaminant exposure types are pooled together in an LDA analysis. These observations agree well with previously reported data, regarding biochemical and even photochemical data of diatom exposure to Cu when compared to other stressors, where a highly toxic effect of this element at certain concentrations was observed, even when compared with other metallic exposures (Cabrita et al., 2018, 2016; Duarte et al., 2021c). Having in mind the high discriminative resolution power of this approach, a similar LDA approach was undertaken for each of the contaminants tested individually, within the proposed range of concentrations. The individual contaminant LDA analysis, revealed very little overlap between samples exposed to different concentrations, indicating once again a high discriminatory power of the variable fluorescence profiles. Some overlap could be observed between some groups, but this was more evident in only two kinds of situations: i) very low concentrations, at which the tested contaminant led to very small or no effects on the diatom photophysiology; ii) high concentrations above the threshold, from which the cells cannot respond proportionally to the dose, either due to complete impairments at different metabolic levels or due to the limit to which the cells can respond has been surpassed. Once again and comparing these overlapping groups with the biochemical responses previously studied, aligns with the detected oxidative stress responses of the cells (Pires et al., 2021), as well as with other metabolic traits (Cruz de Carvalho et al., 2020b; Duarte et al., 2020a; Duarte et al., 2019; Feijão et al., 2020; Franzitta, 2020; Silva et al., 2020). Although this overlap could be considered as a negative aspect of this approach, it reveals the same tendencies previously detected at the biochemical level and thus reinforces the discriminatory power of the whole variable fluorescence to detect exposure groups. Furthermore, it is possible to observe a high degree of efficiency in almost all contaminants tested and for most of the concentrations applied, observing the blind-test classification efficiencies provided by the LDA approach. Thus, this supports the use of the discriminant coefficients provided by the LDA analysis as weighting values within an optical classification tool (OPTOX index), that can integrate the whole variable fluorescence profile. Within the framework of the international OECD guidelines for ecotoxicity bioassays with microalgae (OECD, 2011), the most suitable endpoint to be evaluated in this type of tests is the culture growth inhibition and therefore this trait was used to evaluate the efficiency of the produced index in describing the ecotoxicity resulting for the cells' exposure. Observing the behaviour of the indexes generated for each of the tested contaminants, an increasing index value along with the increasing dose applied was evident, with higher index values attained from the variable fluorescence values correspondent to cultures subjected to the highest exogenous concentrations of each contaminant. In the past, JIP-variables based indexes were already included in unifying numerical indexes revealing a high efficiency in discriminating the stress degree of the test organisms and have been associated with a variety of exogenous stressors ranging from natural (Duarte et al., 2017) to anthropogenic sources (Cruz de Carvalho et al., 2020a; Duarte et al., 2021a). Nevertheless, this is the first time the whole fluorescence dataset profile is integrated into a single descriptor value. Comparing the index numerical value at each condition with the measured growth inhibition and with the effective exogenous dose applied, several strong correlations were evident. Given the negative nature of the growth inhibition variable, most of the correlations were found to be inverse with the calculated index value (higher index values in samples with negative growth values). The exception was observed in the cultures exposed to Cu, where a growth promotion (as observable in the growth inhibition values) occurred and thus a direct correlation was obtained. Nevertheless, a highly positive correlation was found between the index value and the exogenous Cu concentration, indicating a dose–response effect on the photochemical index.

5. Conclusions

The demand for monitor coastal contamination supports the development of innovative tools to evaluate the impacts of contaminants correctly and efficiently in the marine biota, in fast, reliable, and efficient ways. Bio-optical assessments have proved to be an efficient high-throughput screening tool to evaluate marine autotrophs stress level, while providing noteworthy metabolic insights. In the present study, we developed a LDA-based toxicophenomic index, an unifying index enclosing all the fluorescence data provided by the chlorophyll *a* induction curve. The index proved to be an efficient tool for ecotoxicological assays with marine model diatoms and evidenced a high degree of reliability for classifying the exposure of the cells to emerging contaminants. Beyond the obvious potential of the generated indexes for future ecotoxicological assessments, the present work, and the developed methodology, also points to a possible application of similar approaches in other stress physiology studies. The data analysis pipeline, as well as the index development methodology here proposed, can be easily transposed to other autotrophic organisms, subjected to different stress conditions, once calibrated, and validated against known biochemical or morphological descriptors of stress, integrating in this way a large amount of data that was until now completely overlooked and left unrealized in an undervalued dark box.

CRediT authorship contribution statement

Bernardo Duarte: Resources, Conceptualization, Writing - original draft, Data curation, Project administration. **Eduardo Feijão:** Methodology, Investigation. **Ricardo Cruz de Carvalho:** Methodology, Investigation. **Marco Franzitta:** Methodology, Investigation. **João Carlos Marques:** Writing - review & editing. **Isabel Caçador:** Writing - review & editing. **Maria Teresa Cabrita:** Writing - review & editing. **Vanessa F. Fonseca:** Supervision, Funding acquisition, Project administration, Writing - review & editing.

Declaration of Competing Interest

The authors declare that they have no known competing financial interests or personal relationships that could have appeared to influence the work reported in this paper.

Acknowledgements

The authors would like to thank Fundação para a Ciência e a Tecnologia (FCT) for funding the research via project grants PTDC/MAR-EST/3048/2014 (BIOPHARMA), PTDC/CTA-AMB/30056/2017 (OPTOX) and UIDB/04292/2020. B. Duarte and V. F. Fonseca were supported by researcher contracts (CEECIND/00511/2017 and DL57/2016/CP1479/CT0024). M. T. Cabrita is also supported by a DL-57 researcher contract.

References

Anjum, N.A., Duarte, B., Caçador, I., Sleimi, N., Duarte, A.C., Pereira, E., 2016. Biophysical and Biochemical Markers of Metal/Metalloid-Impacts in Salt Marsh Halophytes and Their Implications. Front. Environ. Sci. 4 https://doi.org/10.3389/fenvs.2016.00024.

Cabrita, M.T., Duarte, B., Gameiro, C., Godinho, R.M., Caçador, I., 2018. Photochemical features and trace element substituted chlorophylls as early detection biomarkers of metal exposure in the model diatom Phaeodactylum tricornutum. Ecol. Ind. 95, 1038–1052. https://doi.org/10.1016/j.ecolind.2017.07.057.

Cabrita, M.T., Gameiro, C., Utkin, A.B., Duarte, B., Caçador, I., Cartaxana, P., 2016. Photosynthetic pigment laser-induced fluorescence indicators for the detection of changes associated with trace element stress in the diatom model species Phaeodactylum tricornutum. Environ. Monit. Assess. 188, 285. https://doi.org/10.1007/s10661-016-5293-4.

CAS, 2011. CAS REGISTRY Keeps Pace with Rapid Growth of Chemical Research, Registers 60 Millionth Substance. Chemical Abstracts Service, Columbus.

Cruz de Carvalho, R., Feijão, E., Kletschkus, E., Marques, J.C., Reis-Santos, P., Fonseca, V. F., Papenbrock, J., Caçador, I., Duarte, B., 2020a. Halophyte bio-optical

phenotyping: A multivariate photochemical pressure index (Multi-PPI) to classify salt marsh anthropogenic pressures levels. Ecol. Ind. 119, 106816. https://doi.org/10.1016/j.ecolind.2020.106816.

Cruz de Carvalho, R., Feijão, E., Matos, A.R., Cabrita, M.T., Novais, S.C., Lemos, M.F.L., Caçador, I., Marques, J.C., Reis-Santos, P., Fonseca, V.F., Duarte, B., 2020b. Glyphosate-based herbicide toxicophenomics in marine diatoms: Impacts on primary production and physiological fitness. Applied Sciences (Switzerland) 10, 1–21. https://doi.org/10.3390/app10217391.

Duarte, B., Cabrita, M.T., Vidal, T., Pereira, J.L., Pacheco, M., Pereira, P., Canário, J., Gonçalves, F.J.M., Matos, A.R., Rosa, R., Marques, J.C., Caçador, I., Gameiro, C., 2018. Phytoplankton community-level bio-optical assessment in a naturally mercury contaminated Antarctic ecosystem (Deception Island). Marine Environmental Research 140, 412–421. https://doi.org/10.1016/j.marenvres.2018.07.014.

Duarte, B., Caçador, I., Marques, J.C., Croudace, I.W., 2013. Tagus estuary salt marshes feedback to sea level rise over a 40-year period: Insights from the application of geochemical indices. Ecol. Ind. 34, 268–276. https://doi.org/10.1016/j.ecolind.2013.05.015.

Duarte, B., Durante, L., Marques, J.C., Reis-Santos, P., Fonseca, V.F., Caçador, I., 2021a. Development of a toxicophenomic index for trace element ecotoxicity tests using the halophyte Juncus acutus: Juncus-TOX. Ecol. Ind. 121, 107097. https://doi.org/10.1016/j.ecolind.2020.107097.

Duarte, B., Feijão, E., Cruz de Carvalho, R., Duarte, I.A., Silva, M., Matos, A.R., Cabrita, M.T., Novais, S.C., Lemos, M.F.L., Marques, J.C., Caçador, I., Reis-Santos, P., Fonseca, V.F., 2020a. Effects of Propranolol on Growth, Lipids and Energy Metabolism and Oxidative Stress Response of Phaeodactylum tricornutum. Biology 9, 478. https://doi.org/10.3390/biology9120478.

Duarte, B., Gameiro, C., Matos, A.R., Figueiredo, A., Silva, M.S., Cordeiro, C., Caçador, I., Reis-Santos, P., Fonseca, V., Cabrita, M.T., 2021b. First screening of biocides, persistent organic pollutants, pharmaceutical and personal care products in Antarctic phytoplankton from Deception Island by FT-ICR-MS. Chemosphere 274, 129860. https://doi.org/10.1016/j.chemosphere.2021.129860.

Duarte, B., Gameiro, C., Utkin, A.B., Matos, A.R., Caçador, I., Fonseca, V., Cabrita, M.T., 2021c. A multivariate approach to chlorophyll a fluorescence data for trace element ecotoxicological trials using a model marine diatom. Estuar. Coast. Shelf Sci. 250, 107170. https://doi.org/10.1016/j.ecss.2021.107170.

Duarte, B., Goessling, J.W., Marques, J.C., Caçador, I., 2015. Ecophysiological constraints of Aster tripolium under extreme thermal events impacts: Merging biophysical, biochemical and genetic insights. Plant Physiol. Biochem. 97, 217–228. https://doi.org/10.1016/j.plaphy.2015.10.015.

Duarte, B., Matos, A.R., Caçador, I., 2020b. Photobiological and lipidic responses reveal the drought tolerance of Aster tripolium cultivated under severe and moderate drought: Perspectives for arid agriculture in the mediterranean. Plant Physiol. Biochem. 154, 304–315. https://doi.org/10.1016/j.plaphy.2020.06.019.

Duarte, B., Pedro, S., Marques, J.C., Adão, H., Caçador, I., 2017. Zostera noltii development probing using chlorophyll a transient analysis (JIP-test) under field conditions: Integrating physiological insights into a photochemical stress index. Ecol. Ind. 76, 219–229. https://doi.org/10.1016/j.ecolind.2017.01.023.

Duarte, B., Prata, D., Matos, A.R., Cabrita, M.T., Caçador, I., Marques, J.C., Cabral, H.N., Reis-Santos, P., Fonseca, V.F., 2019. Ecotoxicity of the lipid-lowering drug bezafibrate on the bioenergetics and lipid metabolism of the diatom Phaeodactylum tricornutum. Sci. Total Environ. 650, 2085–2094. https://doi.org/10.1016/j.scitotenv.2018.09.354.

Duarte, I.A., Reis-Santos, P., Novais, S.C., Rato, L.D., Lemos, M.F.L., Freitas, A., Pouca, A. S.V., Barbosa, J., Cabral, H.N., Fonseca, V.F., 2020c. Depressed, hypertense and sore: Long-term effects of fluoxetine, propranolol and diclofenac exposure in a top predator fish. Sci. Total Environ. 712, 136564. https://doi.org/10.1016/j.scitotenv.2020.136564.

Fabbri, E., Franzellitti, S., 2016. Human pharmaceuticals in the marine environment: Focus on exposure and biological effects in animal species. Environ. Toxicol. Chem. 35, 799–812. https://doi.org/10.1002/etc.3131.

Feijão, E., Cruz de Carvalho, R., Duarte, I.A., Matos, A.R., Cabrita, M.T., Novais, S.C., Lemos, M.F.L., Caçador, I., Marques, J.C., Reis-Santos, P., Fonseca, V.F., Duarte, B., 2020. Fluoxetine Arrests Growth of the Model Diatom Phaeodactylum tricornutum by Increasing Oxidative Stress and Altering Energetic and Lipid Metabolism. Front. Microbiol. 11, 1803. https://doi.org/10.3389/fmicb.2020.01803.

Feijão, E., Gameiro, C., Franzitta, M., Duarte, B., Caçador, I., Cabrita, M.T., Matos, A.R., 2018. Heat wave impacts on the model diatom Phaeodactylum tricornutum: Searching for photochemical and fatty acid biomarkers of thermal stress. Ecol. Ind. 95, 1026–1037. https://doi.org/10.1016/j.ecolind.2017.07.058.

Fonseca, V.F., Reis-Santos, P., Duarte, B., Cabral, H.N., Caçador, M.I., Vaz, N., Dias, J.M., Pais, M.P., 2020. Roving pharmacies: Modelling the dispersion of pharmaceutical contamination in estuaries. Ecol. Ind. 115, 106437. https://doi.org/10.1016/j.ecolind.2020.106437.

Franzitta, M., Feijão, E., Cabrita, M.T., Gameiro, C., Matos, A.R., Marques, J.C., Goessling, J.W., Reis-Santos, P., Fonseca, V.F., Pretti, C., Caçador, I., Duarte, B., 2020. Toxicity Going Nano: Ionic versus Engineered Cu Nanoparticles Impacts on the Physiological Fitness of the Model Diatom Phaeodactylum tricornutum. Front. Mar. Sci. 7 https://doi.org/10.3389/fmars.2020.539827.

Gavrilescu, M., Demnerová, K., Aamand, J., Agathos, S., Fava, F., 2015. Emerging pollutants in the environment: Present and future challenges in biomonitoring, ecological risks and bioremediation. New Biotechnol. 32 (1), 147–156. https://doi.org/10.1016/j.nbt.2014.01.001.

Guillard, R.R.L., Ryther, J.H., 1962. STUDIES OF MARINE PLANKTONIC DIATOMS: I. CYCLO$_{TEL}$LA NANA HUSTEDT, AND DETONULA CONFERVACEA (CLEVE) GRAN. Can. J. Microbiol. 8, 229–239. https://doi.org/10.1139/m62-029.

Kalaji, H.M., Govindjee, Bosa, K., Kościelniak, J., Żuk-Gołaszewska, K., 2011. Effects of salt stress on photosystem II efficiency and CO2 assimilation of two Syrian barley landraces. Environ. Exp. Bot. 73, 64–72. https://doi.org/10.1016/j.envexpbot.2010.10.009.

Law, R., Hanke, G., Angelidis, M.O., Batty, J., Bignert, A., Dachs, J., Davies, I., Denga, Y., Duffek, A., Herut, B., Hylland, K., Lepom, P., Leonards, P., Mehtonen, J., Piha, H., Roose, P., Tronczynski, J., Velikova, V., Vethaak, D., 2010. Marine Strategy Framework Directive: Task Group 8 Report Contaminants and pollution effects (No. EUR 24335 EN), Joint Research Centre, European Commission. https://doi.org/10.2788/85887.

Marques da Silva, J., Figueiredo, A., Cunha, J., Eiras-Dias, J.E., Silva, S., Vanneschi, L., Mariano, P., 2020. Using Rapid Chlorophyll Fluorescence Transients to Classify Vitis Genotypes. Plants 9, 174. https://doi.org/10.3390/plants9020174.

OECD, 2011. OECD Guidelines for the testing of Chemicals. Freshwater Alga and Cyanobacteria, Growth Inhibition Test. In: Organisation for Economic Cooperation and Development, pp. 1–25. https://doi.org/10.1787/9789264203785-en.

Pires, V.L., Novais, S.C., Lemos, M.F.L., Fonseca, V.F., Duarte, B., 2021. Evaluation of Multivariate Biomarker Indexes Application in Ecotoxicity Tests with Marine Diatoms Exposed to Emerging Contaminants (preprint). Biology. https://doi.org/10.20944/preprints202103.0735.v1.

Reis-Santos, P., Pais, M., Duarte, B., Caçador, I., Freitas, A., Vila Pouca, A.S., Barbosa, J., Leston, S., Rosa, J., Ramos, F., Cabral, H.N., Gillanders, B.M., Fonseca, V.F., 2018. Screening of human and veterinary pharmaceuticals in estuarine waters: A baseline assessment for the Tejo estuary. Mar. Pollut. Bull. 135, 1079–1084. https://doi.org/10.1016/j.marpolbul.2018.08.036.

Rodrigues, N.M., Batista, J.E., Trujillo, L., Duarte, B., Giacobini, M., Vanneschi, L., Silva, S., 2021. Plotting time: On the usage of CNNs for time series classification. arXiv: 2102.04179 [cs].

Santos, D., Duarte, B., Caçador, I., 2014. Unveiling Zn hyperaccumulation in Juncus acutus: Implications on the electronic energy fluxes and on oxidative stress with emphasis on non-functional Zn-chlorophylls. J. Photochem. Photobiol., B 140, 228–239. https://doi.org/10.1016/j.jphotobiol.2014.07.019.

Silva, M., Feijão, E., da Cruz de Carvalho, R., Duarte, I.A., Matos, A.R., Cabrita, M.T., Barreiro, A., Lemos, M.F.L., Novais, S.C., Marques, J.C., Caçador, I., Reis-Santos, P., Fonseca, V.F., Duarte, B., 2020. Comfortably numb: Ecotoxicity of the non-steroidal anti-inflammatory drug ibuprofen on Phaeodactylum tricornutum. Marine Environmental Research 161, 105109. https://doi.org/10.1016/j.marenvres.2020.105109.

Stirbet, A., Govindjee, 2011. On the relation between the Kautsky effect (chlorophyll a fluorescence induction) and Photosystem II: Basics and applications of the OJIP fluorescence transient. J. Photochem. Photobiol. B 104, 236–257. https://doi.org/10.1016/j.jphotobiol.2010.12.010.

Stirbet, A., Lazár, D., Kromdijk, J., Govindjee, 2018. Chlorophyll a fluorescence induction: Can just a one-second measurement be used to quantify abiotic stress responses? Photosynthetica 56, 86–104. https://doi.org/10.1007/s11099-018-0770-3.

Strasser, R.J., Srivastava, A., Tsimilli-Michael, M., 2000. The fluorescence transient as a tool to characterize and screen photosynthetic samples. In: Probing Photosynthesis: Mechanism, Regulation & Adaptation, pp. 443–480.

Strasser, R.J., Tsimilli-Michael, M., Srivastava, A., 2004. Analysis of the fluorescence transient. In: Papageorgiou, G.C., Govindjee (Eds.), Chlorophyll Fluorescence: A Signature of Photosynthesis. Advances in Photosynthesis and Respiration Series. Springer, Dordrecht, pp. 321–362.

Tsimilli-Michael, M., Eggenberg, P., Biro, B., Köves-Pechy, K., Vörös, I., Strasser, R.J., 2000. Synergistic and antagonistic effects of arbuscular mycorrhizal fungi and Azospirillum and Rhizobium nitrogen-fixers on the photosynthetic activity of alfalfa, probed by the polyphasic chlorophyll a fluorescence transient O-J-I-P. Appl. Soil Ecol. 15 (2), 169–182. https://doi.org/10.1016/S0929-1393(00)00093-7.

Yan, K., Chen, P., Shao, H., Zhao, S., Zhang, L., Zhang, L., Xu, G., Sun, J., 2012. Responses of Photosynthesis and Photosystem II to Higher Temperature and Salt Stress in Sorghum. J. Agron. Crop Sci. 198, 218–225. https://doi.org/10.1111/j.1439-037X.2011.00498.x.